

RESEARCH PAPER

## Substrate Temperature Effect on the Structural and Electrical Properties of SnS Thin Films using prepared Chemical Spray Technique

Rusul K. Mohammed Jasim \*, Raheem G. Kadhim Hussein, and Nassar A. Al-Isawi1

Department of Physics, College of Science, University of Babylon, Iraq

### ARTICLE INFO

**Article History:**

Received 19 July 2022

Accepted 24 September 2022

Published 01 October 2022

**Keywords:**

Chemical spray technique

Electrical properties

I-V characteristics

Structural properties

Tin Sulfide

### ABSTRACT

In this research, The effect of substrate temperature was studied at different temperatures 250, 350 and 450 °C. Structural properties of the films were determined using X-ray diffraction (XRD) and field emission scanning electron microscopy (FESEM). The X-ray diffraction results showed that all the prepared films were polycrystalline, orthorhombic in structure, and a preferred orientation (301),(602) and (111) . The crystallinity of the thin film (SnS) increases with the increase in the temperature (substrate). The electrical properties showed all thin films p-type and D.C conductivity measurements showed that the conductivity increased with increasing temperatures and I-V characteristics were also studied under dark.

### How to cite this article

Jasim R K M., Hussein R G K., Al-Isawi N A. Substrate Temperature Effect on the Structural and Electrical Properties of SnS Thin Films using prepared Chemical Spray Technique. J Nanostruct, 2022; 12(4):859-869. DOI: 10.22052/JNS.2022.04.008

### INTRODUCTION

Thin film technology has been instrumental in providing a clear recognizing of several of the things that make up the world and crystalline structure of the thin films, as well as knowledge of the nature of electronic transitions and their efficiency in the field of application, thanks in part to this technology. Therefore, it has become necessary nowadays to provide materials that have high absorbency. This is because of its importance in the manufacture of solar cells, gas sensors, LEDs, as well as photo electronic and piezoelectric gadgets. one of these materials is tin sulfide. Tin sulfide is a good absorbent layer for solar cells [1]. It is a good energy source, economically, is available in the ground, is non-toxic and has a high optical absorption coefficient

(>10<sup>4</sup> cm<sup>-1</sup>) and high hole mobility (90 cm<sup>2</sup> V<sup>-1</sup>s<sup>-1</sup>) and quantum yield for the excited carrier and low recombination velocity. It has the ionization energy of 4.7 eV, work function of 4.2 eV and an electron affinity of 3.59 eV. The selection of ohmic contact for SnS films is easy because of its lower work function [2,3]. It has a layer structure similar to that of compounds like tin selenide (SnSe), germanium sulfide (GeS), and germanium selenide (GeSe). Because of their layered architectures and strong anisotropic vibrational characteristics, SnS materials display notable changes in their physical characteristics when measured along their crystallographic axes [4]. It exhibits both type and n-type conductivity depending on the tin and sulfur concentration and with temperature treatment [5]. SnS has a consistent low-symmetric,

\* Corresponding Author Email: [usulkadhom7@gmail.com](mailto:usulkadhom7@gmail.com)



This work is licensed under the Creative Commons Attribution 4.0 International License.

To view a copy of this license, visit <http://creativecommons.org/licenses/by/4.0/>.

double-layered orthorhombic crystal structure with lattice parameters of  $a = 0.4329$ ,  $b = 1.1192$ , and  $c = 0.3984$  nm. Due to the configuration of the structural lattice with cations and anions, these layer-structured materials are appealing for use in a variety of device applications [6]. SnS the easiest material system compared to other compound semiconductors, such as Cu (In,Ga) (S,Se)<sub>2</sub> (CIGS) containing rare metals (In and Ga) or Cu<sub>2</sub>ZnSn (S,Se)<sub>4</sub> (CZTS) [7], Several ways to manufacture thin films such as chemical spray pyrolysis, sol-gel, bath deposition, electrochemical deposition, atomic layer deposition, etc. [8]. Each method has several advantages and disadvantages, In this research, was used chemical spray pyrolysis technique (CSP). One of the main problems faced while depositing SnS thin films is the formation of multiple phase SnS such as Sn<sub>2</sub>S<sub>3</sub>/SnS<sub>2</sub>/Sn<sub>3</sub>S<sub>4</sub> films [9]. But this method is characterized by being inexpensive, economical, swift, simple preparation, it is used with oxides to obtain high adhesion and large areas of films. In addition, does not need a vacuum system [10]. It is defined as the process of thermal decomposition of the compound "forming a precipitate" of residual materials and stable on a hot substrate by the deposition of a solution of salts of the materials to be prepared after that the films begin to grow with the continuation of the sedimentation process [11]. SnS as one of the IV-VI group compound semiconductors with an orthorhombic structure, is a strong alternative worth developing as a photovoltaic absorber

owing to its suitable band gap (1.2-1.6 eV) that lies between Silicon and germanium that enable SnS thin films to be used as absorber layer in the fabrication of photovoltaic devices [12].

## MATERIALS AND METHODS

The spray solutions were prepared from a substance Stannous chloride (SnCl<sub>2</sub>·2H<sub>2</sub>O) (with a weight of 22.6.g), and from thiourea (CS(NH<sub>2</sub>)<sub>2</sub>) (with a weight of 7.6 g) Standard (0.1 M). The substances were dissolved in (100 ml of distilled water). The required weights were calculated using a sensitive balance The (Mettler) type has a maximum capacity of 0.16 kg. After completing the dissolution process and obtaining the appropriate solution, the solution is left for some time and then filtered well with filter paper until we obtain a clear, homogeneous solution free of plankton and ready for spraying.

Then The spraying process takes place at temperatures (250,350 and 450)°C on glass panels with dimensions of (2.54-2.54) cm. The deposition process by chemical spray technique is shown in Fig. 1. The distance from the nozzle to the base is (25) cm and the diameter of the nozzle is (0.2) mm. It contains a cylindrical tank with a capacity of (150)ml, open from the top with a radius of (1.5)cm and a height of (10) cm. This tank is used to put the solution to be sprayed. The air pressure inside the glass room was adjusted to obtain a fine atomizer in order to avoid the rapid decrease in substrate temperature which will cause the

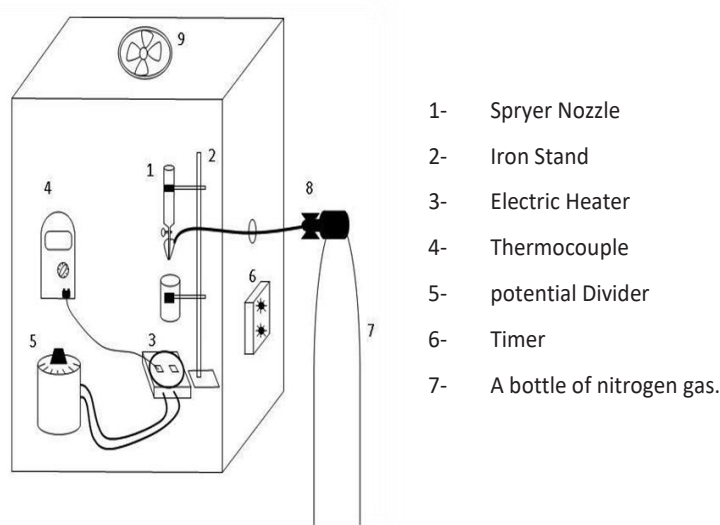
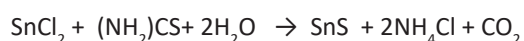


Fig. 1. Diagram of Chemical Spray Pyrolysis

glass substrate to be broken. In this work, the air pressure was kept at (105 N/m<sup>2</sup>) to get uniform films. After that, the plates are lifted from the surface of the heater, and thus a thin, cohesive film is obtained, free of stains, with a smooth surface, and with high adhesion strength with the glass. The films are homogeneous and do not contain dark and light areas. So the solution is sprayed with compressed air for a period of (4s), then followed by a pause for (1)min to ensure that the required base temperature is reached, then another spray is followed for (4s). During cooling, no stress occurred during the sedimentation process, ensuring a homogeneous, spot-free thin film with high adhesion to the base. The SnS film with thickness (200) nm and measured by by ellipsometry (Nano Cal 2000) in the University of Tehran.

SnS film forms according to the following reaction [13]:



Chemical techniques for the preparation of thin films consist of several simple devices as shown in Fig. 1.

## RESULTS AND DISCUSSION

### Structural properties of SnS

#### X-Ray Diffraction Analysis (XRD)

XRD patterns of the SnS films deposited on

glass substrate at different temperatures (250,350 and 450) °C are shown in Fig. 2. The XRD peaks have been discovered at  $2\theta=31.7^\circ$  and  $2\theta=38.5^\circ$ . According to card number 26-0575 from the International Center of Diffraction Data (ICDD). The strongest peak is at  $2\theta=31.7^\circ$ , which is known as the preferred plane (301). We can be noticed that all the patterns exhibit diffraction peaks around ( $2\theta=31^\circ, 16.2^\circ, 21.4^\circ, 26.7^\circ,$  and  $44.7^\circ$ ) referred to (111), (301), (311),(411), and (602) favourite directions respectively as shown in Table 1. The positions of the peaks and the presence of more than one diffraction peak lead to the conclusion that the films are polycrystalline with an orthorhombic crystalline structure when the temperature of the substrate rises, the mobility of the atoms on the surface rises, allowing them to rearrange their locations to occupy more stable places. For all films, the crystallite size was calculated from (FWHM) ( $\beta$ ) of the preferred orientation diffraction peak by using the Debye-Sherre' s equation [14,15]. These results are in agreement with previous research [16][17].

#### Field Scanning Electron Microscopy Analysis (FESEM)

The morphology of a surface in which SnS films grow at different temperatures is analyzed with FESEM and the samples are shown in Fig. 3. The surface has the same shapes of grains with grain boundaries. With increasing the temperature

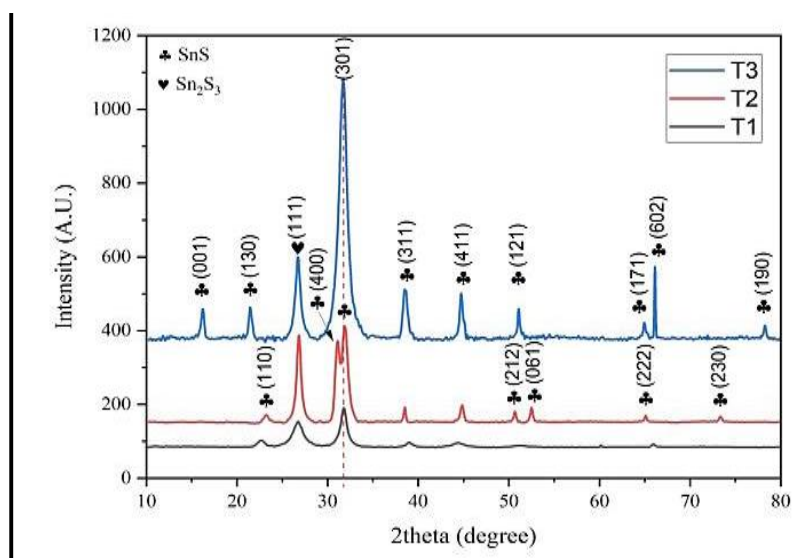


Fig. 2. X-ray diffraction (XRD) pattern of SnS thin film at 250,350 and 450 °C

Table 1. Experimental XRD data for SnS films at 250,350 and450 °C.

Substrate Temperature TS (°C)	(hkl)	2θ (Deg.) Std	2θ (Deg.) Exp	d <sub>hkl</sub> Exp (nm)	d <sub>hkl</sub> Std. (nm)	FWHM (rad)	D (nm)	Average D (nm)
250	(110)	22.667	22.731	3.9197	3.90887	0.933	8.8	15.675
	(111)	26.732	26.587	3.33215	3.35	1.331	6.2	
	(301)	31.781	31.666	2.81338	2.82335	0.816	10.2	
	(311)	39.019	39.096	2.30656	2.3022	0.856	9.9	
	(411)	44.409	44.792	2.03829	2.02175	1.603	5.4	
	(212)	51.166	50.719	1.78385	1.79853	2.15	4.1	
	(170)	60.164	60.623	1.53678	1.52626	0.169	57	
	(222)	65.957	65.919	1.41515	1.41588	0.406	23.8	
	(110)	22.909	22.731	3.87879	3.90887	0.871	9.4	
	(111)	26.827	26.587	3.32054	3.35	0.577	14.4	
350	(400)	31.066	31.666	2.8765	2.82335	0.548	15.3	23.88
	(301)	31.903	31.987	2.80284	2.79575	0.827	10.1	
	(311)	38.527	39.096	2.33484	2.3022	0.23	37.9	
	(411)	44.845	44.792	2.0195	2.02175	0.393	22.3	
	(212)	50.676	50.719	1.79995	1.79853	0.274	33	
	(061)	52.508	52.591	1.74137	1.73882	0.326	27.9	
	(222)	65.094	65.504	1.43181	1.42384	0.249	39.1	
	(230)	73.363	73.335	1.28949	1.28991	0.345	29.4	
	(001)	22.909	22.731	3.87879	3.90887	0.3424	24	
	(130)	26.827	26.587	3.32054	3.35	0.3625	22.8	
450	(111)	31.066	31.666	2.8765	2.82335	0.6244	13.3	27.35
	(3 01)	16.2288	16.239	5.45731	5.454	1.0754	7.7	
	(311)	21.4677	21.499	4.13591	4.13	0.5237	16.3	
	(411)	26.7295	26.587	3.33247	3.35	0.4028	21.7	
	(121)	31.7086	31.666	2.81962	2.82335	0.2618	34.7	
	(171)	38.5899	39.096	2.33119	2.3022	0.3424	28.2	
	(602)	44.7496	44.792	2.02357	2.02175	0.1424	70.7	
	(190)	51.085	51.177	1.78649	1.7835	0.3084	34.1	

there is a change in the grain boundaries as well as the grain size. When the films are deposited at setting up substrate temperature of (250) °C it can be seen that the particles are elongated and

randomly the surface appears rougher. From the SEM images, the average size of the grains is (34.7, 26.6 and 25.3) nm at (250,350 and 450)°C. At (450) °C the crystallites are packed densely and grown



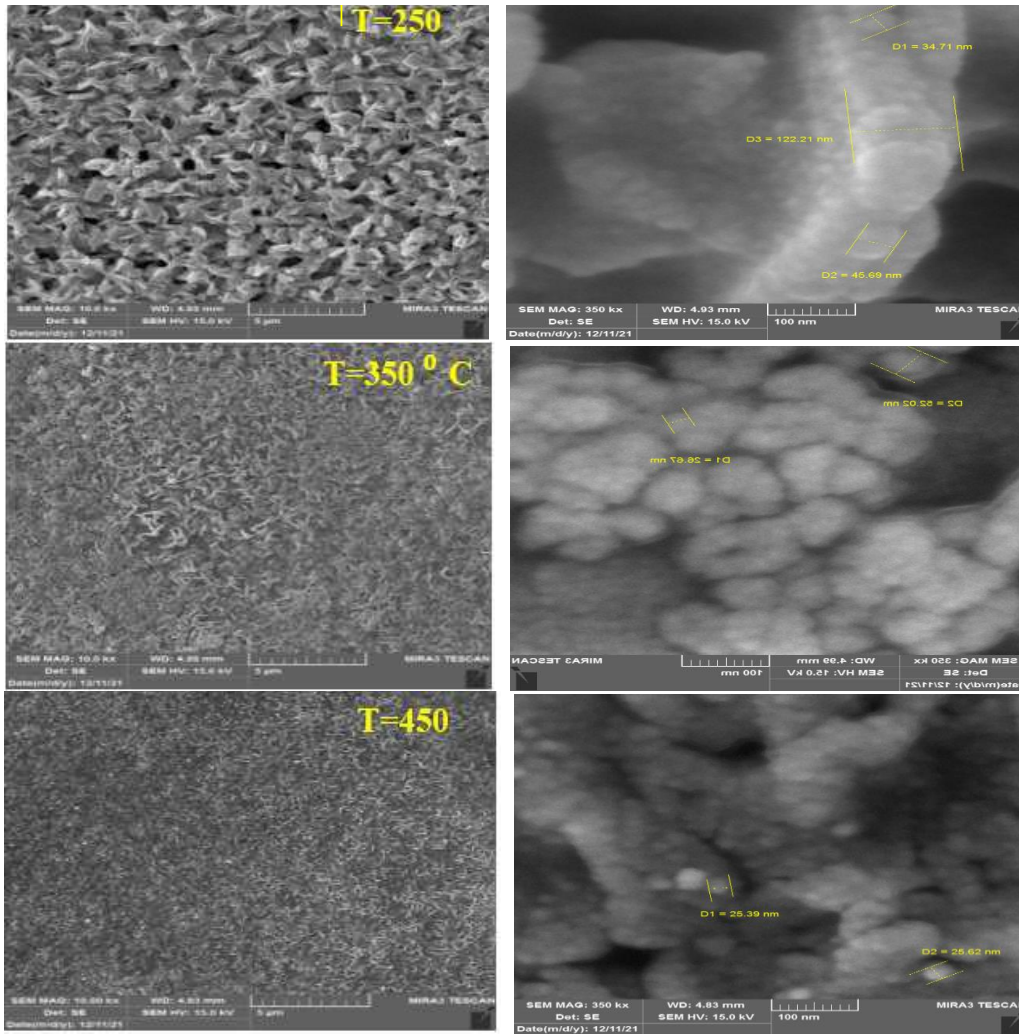


Fig. 3. FESEM images of the SnS thin films at 250,350 and 450 °C

with various sizes in different directions and it is seen that it has pinhole-free, smoother, and more

homogeneous film surface than films sprayed at lower temperatures. The granular surface

Table 2. Hall parameters for SnS thin films.

Substrate Temperature ° C	$R_H$ ( $\text{cm}^3/\text{C}$ )	$\rho_H$ ( $1/\text{cm}^3$ )	$(\sigma_{D.C})_{R.T}$ ( $\Omega.\text{cm}$ ) <sup>-1</sup>	$\rho_{R.T}$ ( $\Omega.\text{cm}$ )	$\mu_H$ ( $\text{cm}^2/\text{V.s}$ )
250	3.348E+7	2.447E+11	1.640E-5	6.097E+4	4.184 E +2
350	2.514E+7	1.236E+12	6.174E-5	1.620E+4	3.117E+2
450	5.705E+6	1.036E+11	6.489-5	1.541E+4	3.909E+3

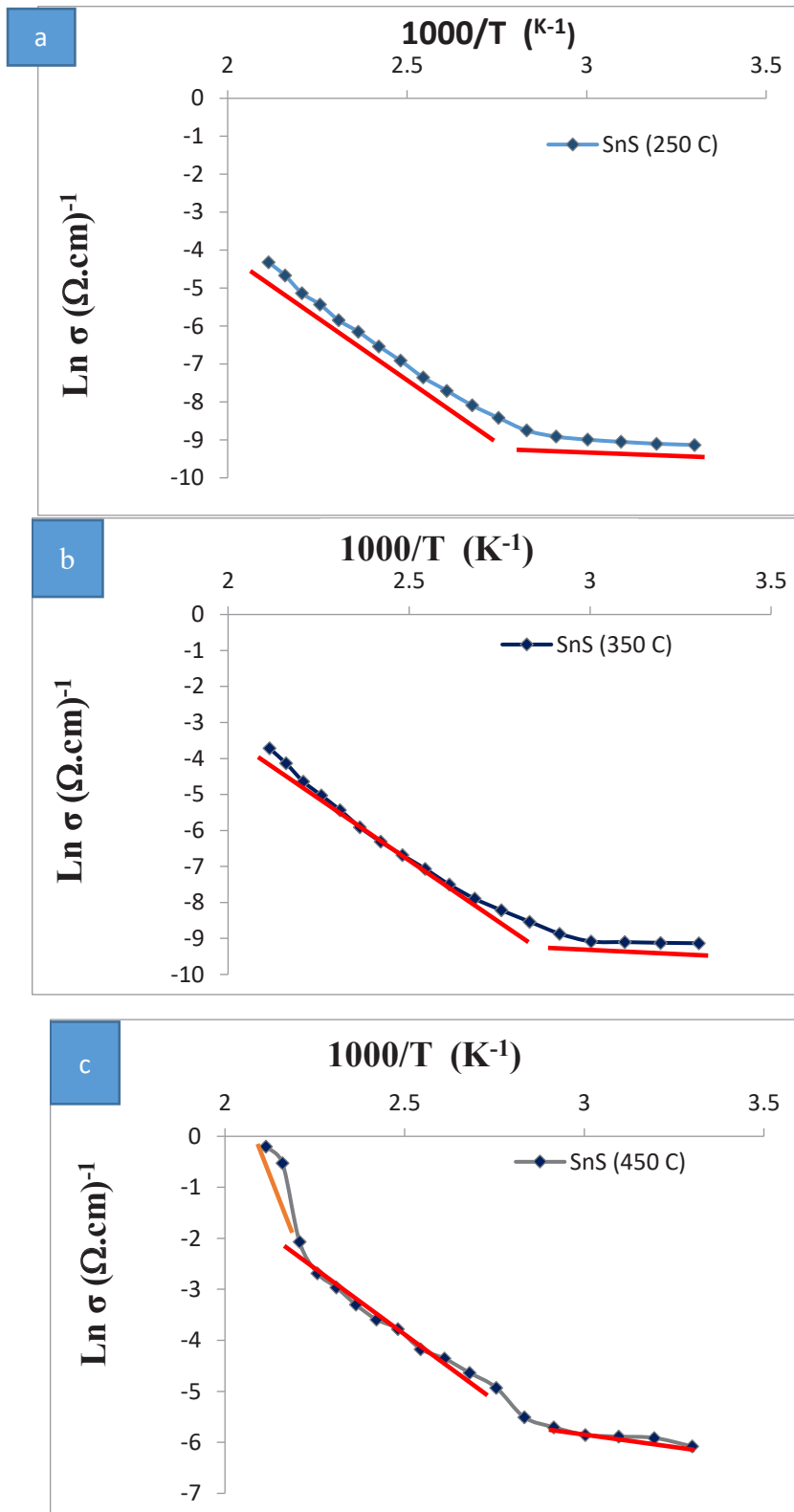


Fig. 4.  $\text{Ln } \sigma$  versus  $1000/T$  for SnS thin films :(a) 250°C (b) 350°C (c) 450° C.

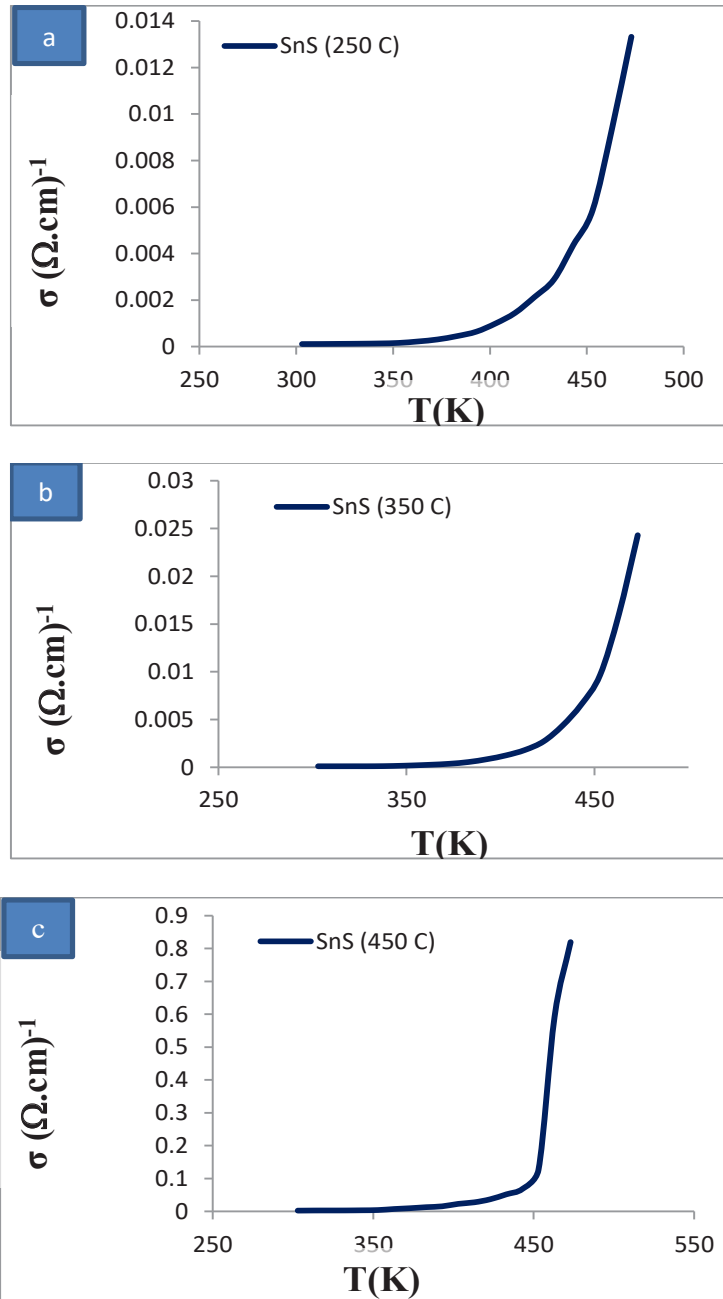


Fig. 5. Variation of  $\sigma_{dc}$  versus temperature for for SnS thin films at (a) 250°C (b) 350°C (c) 450° C.

structure vanished at higher temperatures (350°C and 450°C), and the films became thicker and more compact. The decrease in surface defects and holes and the appearance of grain borders clearly indicates an improvement in the crystalline structure of the film and means an improvement in the properties of the film. These results are in

agreement with previous research [10,16].

#### *The Electrical Properties of SnS thin films Hall Effect Measurements*

All of the produced films had p-type conductivity, according to Hall Effect tests (RH) is determined by the magnitude of an incident

Table 3. D.C. conductivity parameters for SnS thin films.

Substrate Temperature °C	$E_{a1}$ ( eV)	Temp. Range (K)	$E_{a2}$ (eV)	Temp. Range (K)
250	0.3850	(383-303)	0.0921	(383-473)
350	0.6329	(383-303)	0.1373	(383-473)
450	0.5358	(383-303)	0.4875	(383-473)

magnetic field on a film that is placed vertically in front of it. The key parameters derived from Hall Effect measurements, which provide positive RH values, are shown in Table 2. Concentration (nH), Hall mobility ( $\mu_H$ ), conductivity ( $\sigma$ ), and resistivity ( $\rho$ ) are all types of charge carriers. The mobility increased in the sample at (350)°C, despite the fact that the carrier concentration and resistivity dropped. Furthermore, when the sample was heated to 450°C, the carrier concentration and resistivity rose, whereas mobility dropped. The existence of disorder, high density of state, and structural flaws in the film might explain the high resistivity of the as-deposited samples [18], for example. The carrier concentration dropped when the sample was at (450)°C. Furthermore, due of the enhanced mobility, the resistance was reduced and the conductivity rose. These results are in agreement with previous research [18,19].

#### D.C conductivity

The value of electrical conductivity was calculated as a function of the temperature of SnS thin films deposited on glass and is displayed in Table 3. It can be noted that there is an increase in the conductivity values with the increase in the substrate temperature, Where the carriers need high activation energy  $E_a$  to transport them from V.B to C.B and vice versa. It is suitable to determine in the intrinsic range the activation energies and in the extrinsic range the main energy gap. By Plot logarithm of the conductivity ( $\ln \sigma$ ) as a function of  $1000/T$ , by taking the slope of straight lines of  $(-\Delta E/k_B)$ . Table 3. shows increased charge carrier concentration when the temperature reached 450°C to be less than that of the film deposited at 250°C. the conductivity increased with increasing the temperatures and decreased the conductivity increased with  $1000/T$ . It can be noted that there is an increase in the conductivity values with the increase in the substrate temperature, Where the

carriers need high activation energy  $E_a$  to transport them from V.B to C.B and vice versa. It is suitable to determine in the intrinsic range the activation energies and in the extrinsic range the main energy gap. By Plot logarithm of the conductivity ( $\ln \sigma$ ) as a function of  $1000/T$ , by taking the slope of straight lines of  $(-\Delta E/k_B)$ . From Fig. 4., it is discovered that there is two-stage of conductivity. The first activation energy ( $E_{a1}$ ) at a lower temperature range (308-383) K, the conduction mechanism is due to the carrier excited into the extended states beyond the mobility edge and the second activation energy ( $E_{a2}$ ) occurs at a higher temperature range (383-473) K, the conduction mechanism is due to carrier excited into localized states at the edge of the band. These results are in agreement with previous research [19,20].

#### Current-Voltage Characteristic of SnSHeterojunction

Fig. 5 shows the current-voltage(I-V) characteristics of SnS heterojunctions in the dark state of the heterojunction manufactured with different base temperatures (250,350, and 450) in the cases of forward and reverse bias. As we note that the results showed a wave-like behavior in a symmetrical manner, in the forward and reverse directions. Fitting has also been done, it was represented by a straight line, which means that the relationship between current and voltage was linear according to the results announced in. Thus, the concentration of the majority and minority carriers is greater than the square of the eigenvector concentration ( $n_p < n_i^2$ ) In order to reach the state of equilibrium, a current is created at low voltages called the re-arcending current, and at higher voltages, there is no clear change in the current with the bias voltage and this region is called (Diffusion Region) or (the arcing) and it is also called the series resistance.

In the reverse bias region, the bias voltage



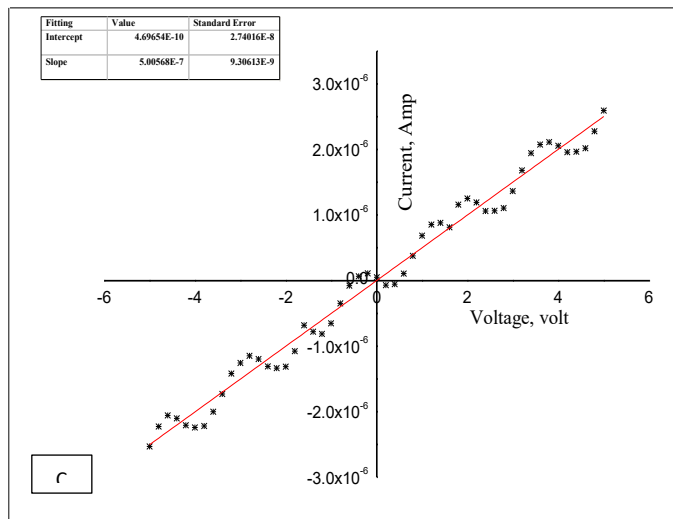
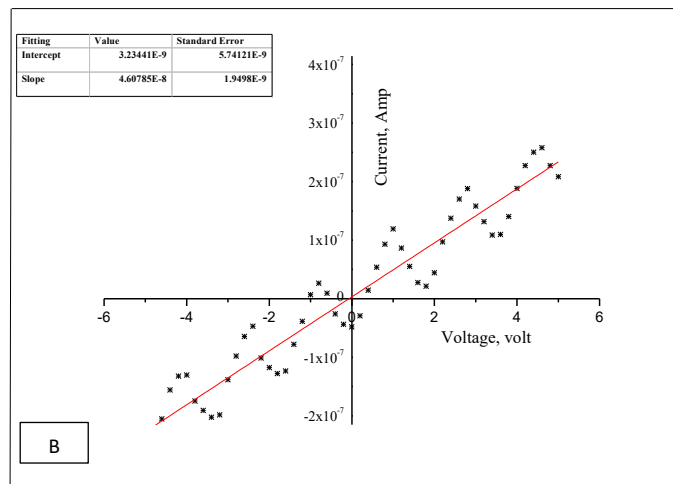
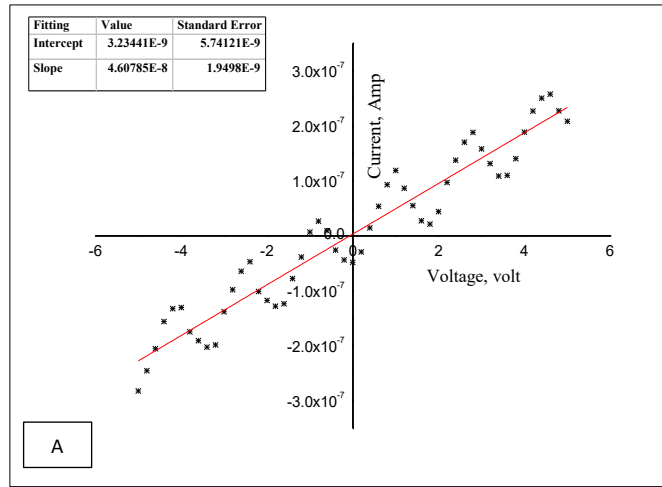


Fig. 6. I-V characteristic for SnS at A) 250 °C, B) 350 °C and C) 450 °C.

increases the width of the depletion region, which leads to a decrease in the concentration of the majority and minority carriers so that their product is less than the square of the auto carrier concentration ( $n_p > n_i^2$ ). In order to reach the state of equilibrium, a current called (Generation Current) At low voltages also, but at higher voltages, the region is called (Diffusion Region). Under dark condition, the current-voltage (I-V) characteristics are important parameter to identify the importance of the various components under reverse and forward bias as well as other important parameters. The I-V characteristic for heterojunctions at forward bias voltage for different temperatures. These results are in agreement with previous research [11,21].

## CONCLUSION

Spray pyrolysis is a good technique in the preparation of thin films. The (XRD) measurements of SnS thin films show that the structures are polycrystalline orthorhombic type. It can be concluded that all the films show a high intense diffraction peak (301) of thin films. As the increase in the average crystallite size with an increase in substrate temperature. SEM images show that the average grain size decrease with increases in the substrate temperature this shows an improvement in the structural properties of the prepared films. The Hall measurements showed that the SnS thin films had p-type conductivity and the Hall coefficient ( $R_H$ ) increased with increasing substrate temperature. The D.C conductivity measurements showed that the conductivity increased with increasing the temperatures because of increased charge carrier concentration and decreased the conductivity with increased with  $1000/T$ . In addition, they have two activation energies. The SnS structure showed the junction behavior as a Schottky diode.

## CONFLICT OF INTEREST

The authors declare that there is no conflict of interests regarding the publication of this manuscript.

## REFERENCES

1. Frey H. Applications and Developments of Thin Film Technology. Handbook of Thin-Film Technology: Springer Berlin Heidelberg; 2015. p. 1-3.
2. Minnam Reddy VR, Gedi S, Park C, R.W M, K.T RR. Development of sulphurized SnS thin film solar cells. CAP. 2015;15(5):588-598.
3. Yue GH, Peng DL, Yan PX, Wang LS, Wang W, Luo XH. Structure and optical properties of SnS thin film prepared by pulse electrodeposition. Journal of Alloys and Compounds. 2009;468(1-2):254-257.
4. Kang J-y, Kwon S-M, Yang SH, Cha J-H, Bae JA, Jeon C-W. Control of the microstructure of SnS photovoltaic absorber using a seed layer and its impact on the solar cell performance. Journal of Alloys and Compounds. 2017;711:294-299.
5. Ninan GG, Sudha Kartha C, Vijayakumar KP. On the preparation of n-type SnS:Cu using chemical spray pyrolysis for photovoltaic application: Effect of annealing. Sol Energy Mater Sol Cells. 2016;157:229-233.
6. Koteswara Reddy N, Devika M, Gopal ESR. Review on Tin (II) Sulfide (SnS) Material: Synthesis, Properties, and Applications. Crit Rev Solid State Mater Sci. 2015;40(6):359-398.
7. Heriche H, Bouchama I, Bouarissa N, Rouabah Z, Dilmi A. Enhanced efficiency of Cu(In,Ga)Se<sub>2</sub> solar cells by adding Cu<sub>2</sub>ZnSn(S,Se)<sub>4</sub> absorber layer. Optik. 2017;144:378-386.
8. Bashkurov SA, Gremenok VF, Ivanov VA, Lazenka VV, Bente K. Tin sulfide thin films and Mo/p-SnS/n-CdS/ZnO heterojunctions for photovoltaic applications. Thin Solid Films. 2012;520(17):5807-5810.
9. Schneikart A, Schimper HJ, Klein A, Jaegermann W. Efficiency limitations of thermally evaporated thin-film SnS solar cells. J Phys D: Appl Phys. 2013;46(30):305109.
10. Sall T, Soucase BM, Mollar M, Sans JA. SnS Thin Films Prepared by Chemical Spray Pyrolysis at Different Substrate Temperatures for Photovoltaic Applications. Journal of Electronic Materials. 2017;46(3):1714-1719.
11. Arepalli VK, Nguyen TD, Kim J. Influence of Ag thickness on the structural, optical, and electrical properties of the SnS/Ag/SnS trilayer films for solar cell application. CAP. 2020;20(3):438-444.
12. Mohan VV, Akshaya KC, Asha AS, Jayaraj MK, Vijayakumar KP. Effect of substrate temperature on the optoelectronic properties of chemically sprayed SnS thin films. Materials Today: Proceedings. 2021;39:1978-1980.
13. Ray SC, Karanjai MK, DasGupta D. Structure and photoconductive properties of dip-deposited SnS and SnS<sub>2</sub> thin films and their conversion to tin dioxide by annealing in air. Thin Solid Films. 1999;350(1-2):72-78.
14. Islam MA, Hossain MS, Aliyu MM, Chelvanathan P, Huda Q, Karim MR, et al. Comparison of Structural and Optical Properties of CdS Thin Films Grown by CSVT, CBD and Sputtering Techniques. Energy Procedia. 2013;33:203-213.
15. Rajendra BV, Bhat V, Kekuda D. Optical Properties of Zinc Oxide (ZnO) Thin Films Prepared by Spray Pyrolysis Method. Advanced Materials Research. 2014;895:226-230.
16. Guneri E, Ulutas C, Kirmizigul F, Altindemir G, Gode F, Gumus C. Effect of deposition time on structural, electrical, and optical properties of SnS thin films deposited by chemical bath deposition. Applied Surface Science. 2010;257(4):1189-1195.
17. Henry J, Mohanraj K, Kannan S, Barathan S, Sivakumar G. Structural and optical properties of SnS nanoparticles and electron-beam-evaporated SnS thin films. J Exp Nanosci. 2013;10(2):78-85.
18. Guneri E, Gode F, Ulutas C, Kirmizigul F, Altindemir G, and Gumus C. Properties of p-type SnS thin films prepared by chemical bath deposition. Chalcogenide Lett. 2010; 7(12): 685-694.

19. Shen S, Bottomley LA. Microcantilever Sensing of Particles in Liquid Streams: Thin-Film Coating Impacts Sensor Performance. *Thin Films: Preparation, Characterization, Applications*: Springer US; 2002. p. 349-359.
20. Ferro R. Some physical properties of F-doped CdO thin films deposited by spray pyrolysis. *Thin Solid Films*. 1999;347(1-2):295-298.
21. Ogah OE, Reddy KR, Zoppi G, Forbes I, Miles RW. Annealing studies and electrical properties of SnS-based solar cells. *Thin Solid Films*. 2011;519(21):7425-7428.